

# Physcion 8-O- $\beta$ -glucopyranoside exhibits anti-growth and anti-metastatic activities in ovarian cancer by downregulating miR-25

C.-L. XUE, H.-G. LIU, B.-Y. LI, S.-H. HE, Q.-F. YUE

Department of Gynaecology, Luoyang Central Hospital Affiliated to Zhengzhou University, Luoyang, Henan, China

**Abstract.** – **OBJECTIVE:** Ovarian cancer ranks 5<sup>th</sup> leading cause of cancer-related death in females worldwide. Physcion 8-O- $\beta$ -glucopyranoside (PG) is an anthraquinone compound isolated from *Rumex japonicus* Houtt. This study aimed at investigating the effect of PG on ovarian cancer cells.

**PATIENTS AND METHODS:** Cell viability was detected by CCK-8 assay. Colony formation assay evaluated whether PG could affect anchorage-independent growth. Whether PG affected cell cycle progression was examined by flow cytometry. The morphological changes caused by PG were visualized by microscopy. Apoptosis was quantitatively analyzed by flow cytometry. The effect of PG on cell migration and invasion was assessed by wound healing and transwell, respectively. The effect of PG on the expression of molecular markers was determined by Western blot. Microarray assay was performed to identify the potential target of PG.

**RESULTS:** Results from the present study showed that PG decreased ovarian cancer cells viability. Colony formation assay also showed that PG suppressed the anchorage-independent growth of SKOV3 and OVCAR-3 cells. PG triggered cell cycle arrest at G1/G0 phase. The pro-apoptotic activity of PG was confirmed by flow cytometry, activation of caspase-3 and PARP, upregulation of Bax and downregulation of Bcl-2. The ability of PG to inhibit migration and invasion was evidenced by a decrease in wound healing and invasive cell number, as well as downregulation of MMP-2 and upregulation of TIMP-3. Microarray and qRT-PCR showed that miR-25 expression was downregulated by PG treatment. Moreover, our results indicated that the anti-cancer activities of PG were augmented by miR-25 knockdown and attenuated by ectopic miR-25 expression.

**CONCLUSIONS:** PG exhibited anti-cancer activity in ovarian cancer by downregulating miR-25.

*Key Words:*

Ovarian cancer, Physcion 8-O- $\beta$ -glucopyranoside, miR-25.

## Introduction

As a common malignancy of the female reproductive system, ovarian cancer ranks 5th among the leading causes of cancer-related death in females worldwide<sup>1</sup>. Due to the lack of warning signs and specific symptoms, patients are mostly diagnosed at a late stage when metastasis has already occurred<sup>2</sup>. At present, the standard treatment for ovarian cancer patients is still cytoreductive surgery after chemotherapy<sup>3</sup>. However, the prognosis of the patient is still poor<sup>4</sup>. Therefore, it is pivotal to develop new therapeutic agents for the treatment of ovarian cancer. MicroRNAs (miRNAs), a class of endogenous non-coding RNAs consisting of 20-22 nucleotides, are involved in the pathogenesis of a variety of human conditions<sup>5</sup>. With regards to human malignancies, mounting studies<sup>6</sup> have showed that miRNAs are involved in the regulation of tumorigenesis, progression, and metastasis in cancer. Interestingly, many miRNAs have been found to promote or suppress the tumor growth or metastasis of ovarian cancer. For instance, Suo et al<sup>7</sup> reported that miR-200a promotes cell invasion and migration of ovarian carcinoma by targeting PTEN. Zhang et al<sup>8</sup> also identified miR-630 as an oncogene, which can promote the proliferation and invasion of epithelial ovarian cancer by targeting KLF6. These results suggested that miRNA can be considered as a promising therapeutic target for ovarian cancer.

*Rumex japonicus* Houtt, a perennial herbal plant in the East part of Asian countries including China, has been utilized as a folk remedy in treating a variety of common human conditions, such as constipation, uterine hemorrhage and dermatitis<sup>9</sup>. The identified active ingredients in *Rumex japonicus* Houtt include anthraquinones, oxanthrones and flavones<sup>10</sup>. Particularly, the an-

ti-neoplastic activities of PG have been studied in various human cancers<sup>10-15</sup>. However, whether PG exhibited anti-cancer activities in ovarian cancer remains unclear. Our data have indicated that PG suppressed cell proliferation and invasion by suppressing miR-25 in ovarian cancer cells.

## Patients and Methods

### *Patients Information and Specimen Collection*

37 cases of esophageal patients who received treatment in our hospital between January 2013 and December 2013 were recruited in this study. The Ethics Committee of the First Affiliated Hospital of Nanjing Medical University given its official approval and all patients signed written consent form. Ovarian cancer tissues and matched normal tissues were collected and stored at -80°C until use.

### *Cell Lines and Cell Culture*

SKOV3 and OVCAR-3 cells, the ovarian cancer cell lines, were provided by the Type Culture Collection of the Chinese Academy of Sciences. Human normal ovarian epithelial cell line (HOSE) was provided by ATCC (Shanghai, China). All of the cells were cultured in Dulbecco's Modified Eagle's Medium (DMEM) (HyClone, South-Logan, UT, USA) supplemented with 10% FEB (HyClone, South-Logan, UT, USA) in a humidified incubator at 37°C with 5% CO<sub>2</sub>.

### *CCK-8 Assay*

The cell viability was examined via CCK-8 kit (Beyotime, Shanghai, China) following PG treatment. Spectrophotometer (Tecan Group Ltd, Männedorf, Switzerland) was applied to detect the absorbance at 450 nm.

### *Colony Formation Assay*

Following PG treatment, cells at a concentration of  $3 \times 10^4$  cells/ml were inoculated into 6-well plates and cultured for two weeks without feeding. Colonies with a diameter > 0.1 mm were photographed using a Nikon Eclipse TE2000-U microscope (Tokyo, Japan) for counting.

### *Cell Cycle Analysis*

$1 \times 10^5$  cells/well concentration of cells were plated out in a 6-well plate and exposed to different concentration of PG for 48 h. After washing

the cells, ice-cold 70% ethanol was utilized to fix the cells for 2 h at 4°C. FACSscan DNA analysis was performed according to the standard protocol.

### *Flow Cytometry Assay*

Apoptosis was assessed using an apoptosis kit (BD Pharmingen, Franklin Lakes, NJ, USA) in accordance with the manufacturer's instructions. Flow cytometer (Beckman Coulter Inc., Brea, CA, USA) was utilized to quantify the apoptotic cell population.

### *Quantitative Real-Time PCR (qRT-PCR)*

Total miRNAs were isolated from cultured cells or tissues using miRcute miRNA isolation kit (DP501) (Tiangen Biotech, Beijing, China). Extracted miRNAs were reversely transcribed to cDNA using High Capacity cDNA Archive Kit (Applied Biosystems, Foster City, CA, USA) and qRT-PCR was conducted using TaqMan PCR kit (Thermo Fisher Scientific, Waltham, MA, USA). The primers were as the following: forward, 5'-ACACTCCAGCTGGGAGGCGGAGACTTG-GGCAA-3'; reverse, 5'-TGTCGTGGAGTCGG-CAATTC-3'. GADPH served as internal control. The comparative  $\Delta$ Ct method (ABPrism software, Applied Biosystems, Foster City, CA, USA) was used to quantify PCR data.

### *Microarray for Expression of miRNAs*

500 ng of total RNA was extracted from 1.0-1.5 mL blood sample and was used for microarray detection, which was marked by biotin-labeled DNA molecule and hybridized, and then washed on the GeneChip Fluidics Station 450 platform. The signal intensity of each chip varies from one another due to different essential backgrounds of chips; thus, for eliminating the calculation error of miRNA expression, raw data were normalized using Robust Multichip Average (RMA), which is an algorithm used for creating an expression matrix from Affymetrix data. To be exact, the raw values of signal intensity were background corrected, log<sub>2</sub> transformed, and subsequently quantile normalized using RMA method. Thereafter, the normalized data were calculated using a linear model. In the microarray assay, differentiated expressed miRNAs were compared using R package limma. Benjamini and Hochberg procedure was performed to adjust the *p*-values; Volcano map and heat map analysis were used to distinguish information between the two groups.

### **Western Blotting**

Briefly, proteins in cell lysates were firstly resolved by sodium dodecyl sulfate-polyacrylamide gel electrophoresis (SDS-PAGE), then transferred to polyvinylidene difluoride (PVDF), and subsequently incubated with the primary antibodies at 4°C overnight. The secondary antibodies used were goat anti-rabbit IgG-HRP and anti-mouse IgG-HRP (Beyotime, Shanghai, China). Positive bands were detected using chemiluminescent substrate (KPL, Guildford, UK), and BandScan software (Glyko, Novato, CA, USA) was utilized to quantify the band densities.

### **miR-25 Knockdown or Overexpression**

The lentiviral construct miR-25 mimic, miR-25 inhibitor and miR-con purchased from Qiagen (Gene Copoeia, Rockville, MD, USA) were used to transfect SKOV3 and OVCAR-3 cells for 48 h using Lipofectamine 3000. qRT-PCR was applied to detect the transfection efficiency.

### **Wound Scratch Assay**

When the cells cultured in the 6-well plate reached 90% confluence, sterile 200  $\mu$ L pipette tip was utilized to scratch cell monolayer. The scratched wound was imaged in three random fields under 100x magnification after 24 hours. The open area at 0 hours and decreased open area after 24 hours were measured to determine cell migration.

### **Transwell Invasion Assay**

Matrigel (8- $\mu$ m pore size; BD Biosciences, Franklin Lakes, NJ, USA) was utilized to pre-coated Transwell plates. Cells ( $2 \times 10^5$  cells/ml) were resuspended in serum-free medium and then 500  $\mu$ l were inoculated into the upper chamber. The lower chamber of Transwell was filled with MEM containing 10% fetal bovine serum (FBS). After 24 hours of incubation, the remaining cells in the upper chamber were cleaned up, invasive cells attached to the lower surface of the membrane were stained with hematoxylin staining solution and photographed at 200 $\times$  magnification.

### **Statistical Analysis**

Data are presented as means  $\pm$ SD. Statistical comparisons were made using one-way analysis of variance (ANOVA) followed by Dunnett's t-test using GraphPad Prism software (GraphPad Software Inc., La Jolla, CA, USA). \* $p < 0.05$  was considered as statistically significant.

## **Results**

### **PG Exhibits Anti-Proliferative Activities in Ovarian Cancer Cells**

The chemical structure of PG was presented in Figure 1A. Whether PG affected the viability of SKOV3 and OVCAR-3 cells were assessed by CCK-8 assay. Following a 24 hours' treatment, the viability of SKOV3 cells was concentration-dependently reduced by PG. The percentage of viable OVCAR-3 cells was decreased to about 82% and 66% by PG at dosages of 5 and 10  $\mu$ M, respectively. Following a 48 hours' treatment, the percentage of viable SKOV3 cells was decreased to about 70% and 50% by PG at dosages of 5 and 10  $\mu$ M, respectively. OVCAR-3 cells presented with higher sensitivity to PG treatment (Figure 1B). Following a 24 hours' treatment, the percentage of viable OVCAR-3 cells was decreased to about 70% and 50% by PG at dosages of 5 and 10  $\mu$ M, respectively. Following a 48 hours' treatment, the percentage of OVCAR-3 cells was decreased to about 50% and 40% by PG at dosages of 5 and 10  $\mu$ M, respectively. Whether PG affected the capability of colony formation was also examined. As shown in Figure 1C, the number of formed colonies of SKOV3 cells was decreased to about 60% and 50% relative to control by PG at dosages of 5 and 10  $\mu$ M, respectively. As for OVCAR-3 cells, the number of formed colonies was decreased to about 45% and 25% relative to control by PG at dosages of 5 and 10  $\mu$ M, respectively. Next, whether PG affected the cell cycle progression was determined. Following a 48 hours' treatment, the SKOV3 cells in G0/G1 phase were increased from about 50% to about 60% and 70% by PG at dosages of 5 and 10  $\mu$ M, respectively (Figure 1D). The OVCAR-3 cell population in G0/G1 phase was also dose-dependently by PG treatment (Figure 1D).

### **PG Promotes Apoptosis in Ovarian Cancer Cells**

Whether PG was able to cause morphological changes in ovarian cancer cells were examined under microscopy. Treatment with PG for 48 hours significantly affected the shape and reduced adhesive force of both SKOV3 and OVCAR-3 cells (Figure 2A). Next, whether PG affected the apoptotic process of ovarian cancer cells was examined utilizing flow cytometry. Results from flow cytometry showed that PG at dosages of 5 and 10  $\mu$ M increased the apop-

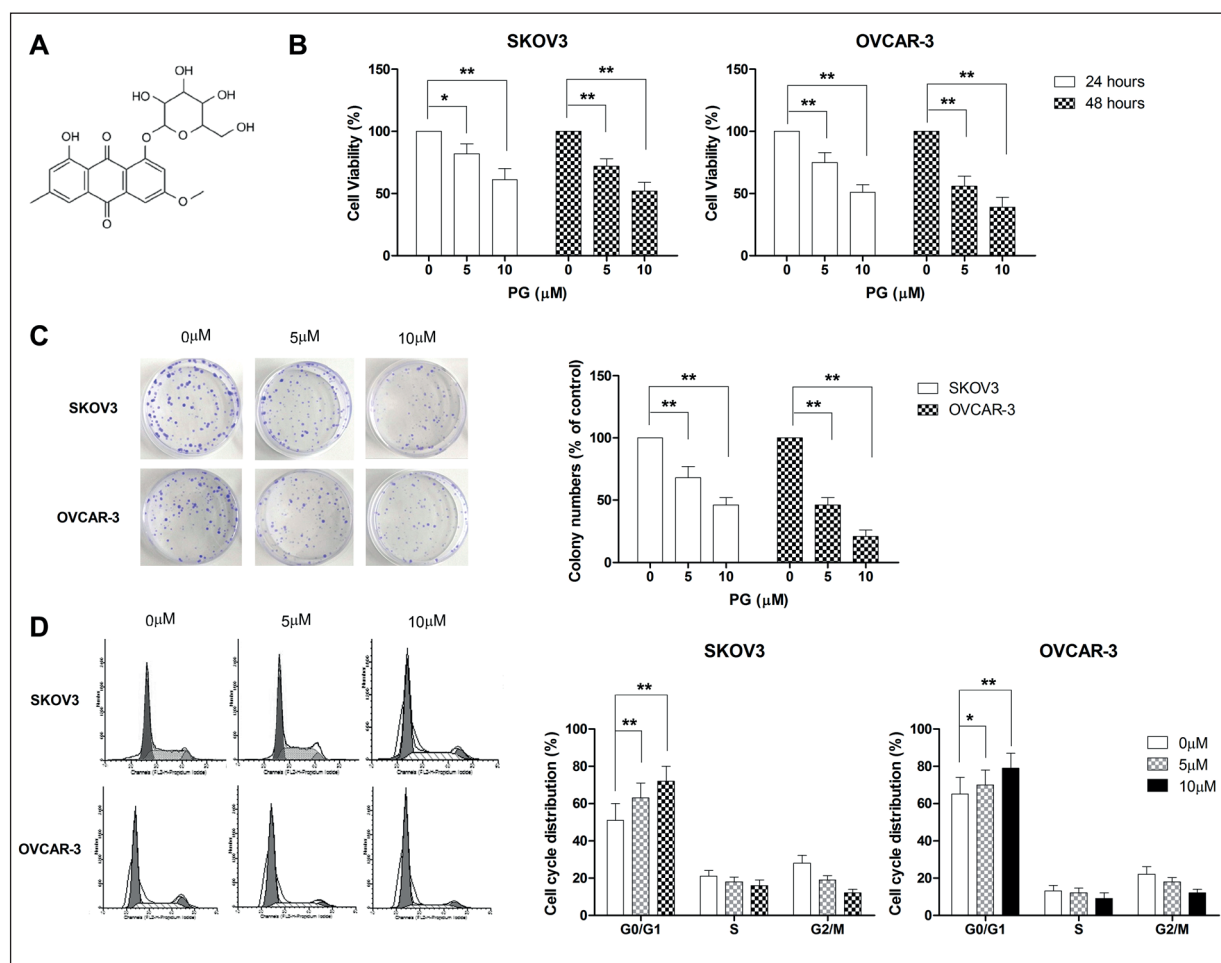


**Figure 1.** PG promotes cell death and suppresses colony formation in SKOV3 and OVCAR-3 cells. *A*, The chemical structure of PG was presented. *B*, The cell viability was assessed by CCK-8 assay. *C*, The effect of PG on colony formation was assessed. *D*, The effect of PG on cell cycle distribution was assessed. \* $p < 0.05$ , \*\* $p < 0.01$ .

totic cell percentage in SKOV3 cells from less than 5% to around 15% and 20%, respectively (Figure 2B). As regards to OVCAR-3 cells, PG treatment at dosages of 5 and 10 μM increased the apoptotic cell population to almost 20% and 30%, respectively (Figure 2B). Following 48 hours' treatment with PG, the levels of activated caspase-3 and PARP were remarkably elevated in SKOV3 and OVCAR-3 cells. Meanwhile, whether PG treatment could affect the expression levels of Bax and Bcl-2 was also examined. Our results indicated that PG treatment down-regulated the expression level of anti-apoptotic molecules Bcl-2. In contrast, the expression level of pro-apoptotic molecules Bax was also upregulated by PG treatment (Figure 2C). Altogether, this evidence showed that PG could promote ovarian cancer cell apoptosis.

### ***PG Suppresses the Migratory and Invasive Abilities of Ovarian Cancer Cells***

Whether PG was able to affect the migratory abilities of ovarian cancer cells was evaluated by performing wounding healing experiments. As shown in Figure 3A, PG exhibited dose-dependent suppressing activities on the migration of both ovarian cancer cell lines. Whether PG was able to affect the invasive ability was evaluated by Transwell assay. Following 24 hours' treatment with PG, the invasive cell number presented a concentration-dependent reduction in SKOV3 and OVCAR-3 cells (Figure 3B). MMP-2 is a key enzyme playing a promoting role in the process of migration and invasion while TIMP-3 is an anti-metastatic molecule. Hence, whether PG affected the expression levels of these two molecules was also determined. As shown in Figure

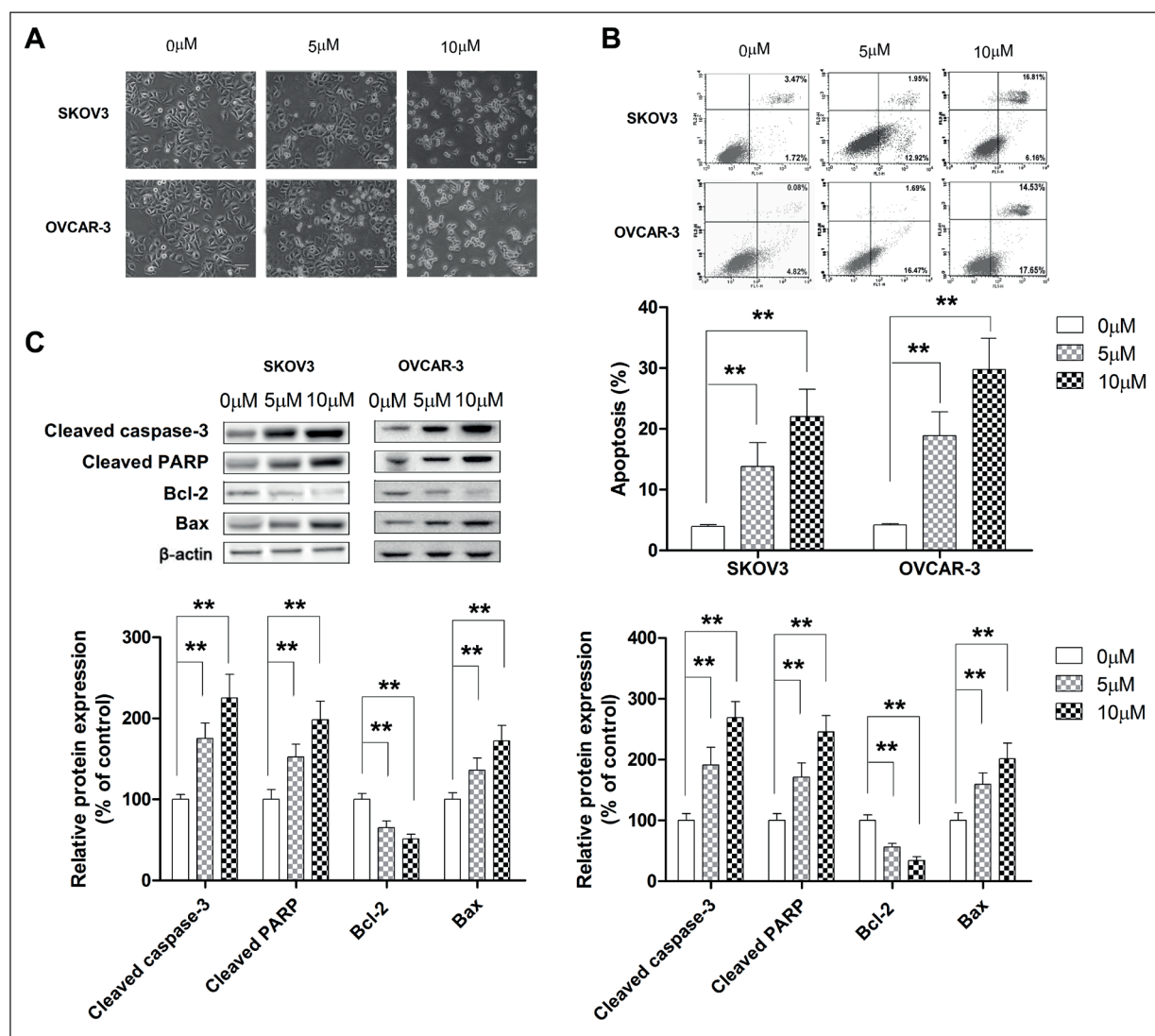


**Figure 2.** PG promotes apoptosis in SKOV3 and OVCAR-3 cells. Cells were treated with PG at 5 and 10  $\mu\text{M}$  for 48 hours. *A*, The morphological change was examined with optical microscopy. *B*, Cells were treated with Annexin V-FITC and apoptotic cell death was detected with flow cytometry. *C*, The cleavage of caspase-3 and PARP, the expression of Bcl-2 and Bax were detected with Western blot. \*\*  $p < 0.01$ .

3C, PG was able to dose-dependently downregulate MMP-2 while upregulating TIMP-3 in both ovarian cancer cells, supporting that PG could suppress the metastasis of ovarian cancer cells.

### PG Represses miR-25 Expression in Ovarian Cancer Cells

A number of studies<sup>16</sup> have proposed that naturally occurring compounds could exhibit anti-cancer activities by upregulating or downregulating miRNAs. In our present study, microarray assay was performed to examine whether PG was able to exert anti-cancer activities by modulating miRNAs. As shown in Figure 4A, our

findings showed that PG was remarkably upregulated and downregulated a number of miRNAs. Among these miRNAs, we focused on miR-25, whose expression level was profoundly reduced following PG treatment. To further examine the effect of PG on miR-25 expression, cells were treated with PG for 48 hours and the expression of miR-25 was detected by qRT-PCR. Our results from qRT-PCR revealed that PG was able to downregulate miR-25 expression (Figure 4B). On the other hand, miR-25 level was significantly higher in ovarian cancer tissues than in matched non-cancerous tissues. Moreover, our findings indicated that the level of miR-25 expression in

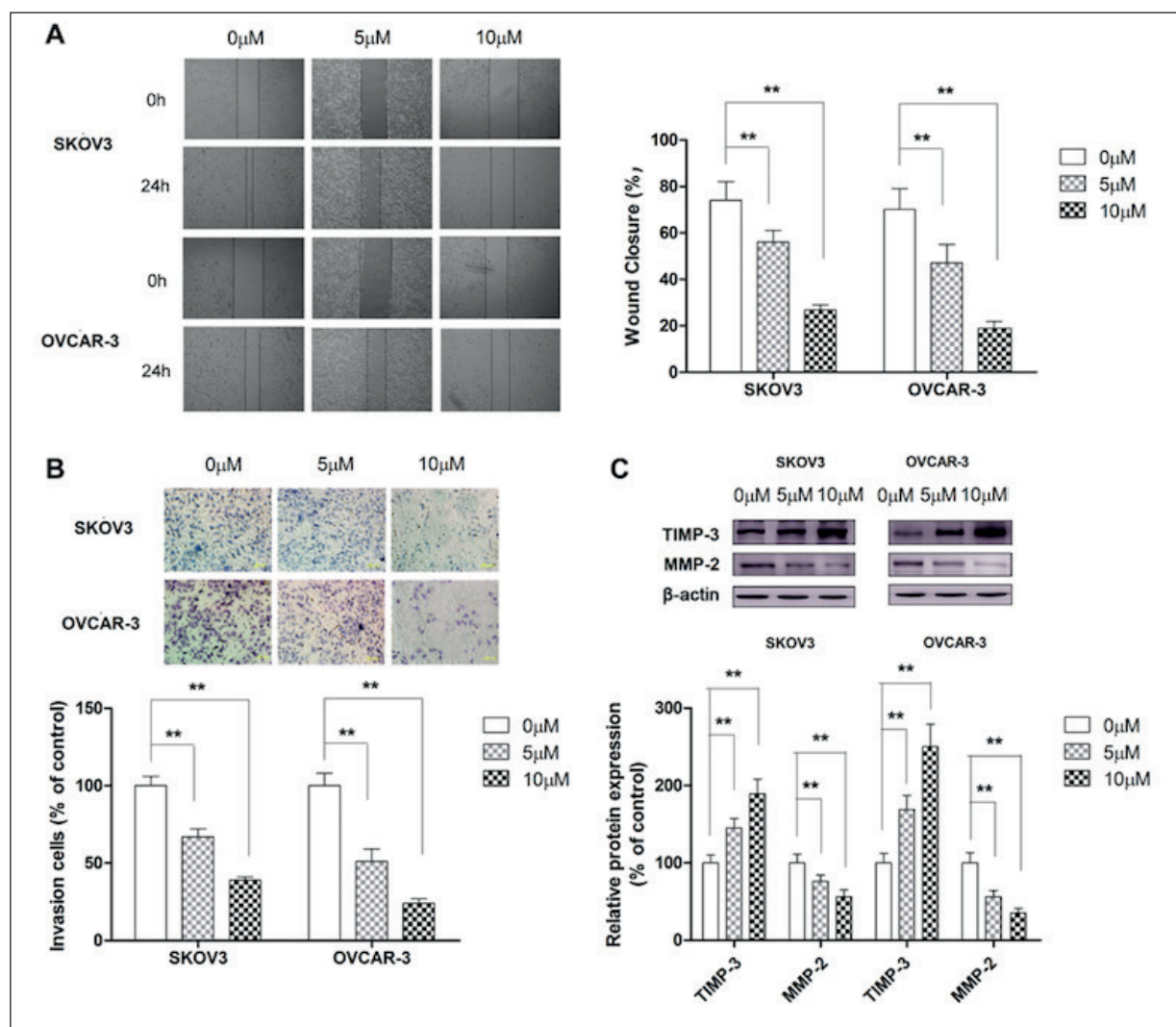


**Figure 3.** PG suppresses migration and invasion of SKOV3 and OVCAR-3 cells. Cells were treated with PG at 5 and 10  $\mu\text{M}$  for 24 hours. **A**, The migration was assessed by performing wound-healing assay. **B**, The cell invasion was assessed by performing transwell assay. **C**, The expression of MMP-2 and TIMP-3 was detected by Western blot. \*\*  $p < 0.01$ .

ovarian cancer cells was significantly higher than in HOSE normal cells (Figure 4D). These combined results demonstrated that miR-25 was an oncogene in ovarian cancer and PG might exert anti-cancer activities by downregulating miR-25.

#### **Forced miR-25 Expression in Ovarian Cancer Cells Compromises the Anti-Cancer Activities of PG**

Given that PG can affect miR-25 expression, ovarian cancer cells were subsequently transfected with miR-25 mimic to introduce ectopic expression of miR-25. The expression level of miR-25 in SKOV3 and OVCAR-3 cells increased more than 2-fold after transfection (Figure 5A).

Then whether ectopic miR-25 expression affected the pro-apoptotic activities of PG was examined. As shown in Figure 5B, the apoptotic cell population was reduced to about 10% in both SKOV3 and OVCAR-3 cells by ectopic miR-25 expression. Furthermore, the activation of caspase-3 and PARP was markedly attenuated by ectopic miR-25 expression. PG-induced downregulation of Bcl-2 was significantly dampened in SKOV3 and OVCAR-3 cells with miR-25 overexpression (Figure 5B). Meanwhile, the upregulation caused by PG treatment was also attenuated by ectopic miR-25 expression (Figure 5C). The effect of ectopic miR-25 expression on cell migration and invasion was also evaluated. As shown in Figure

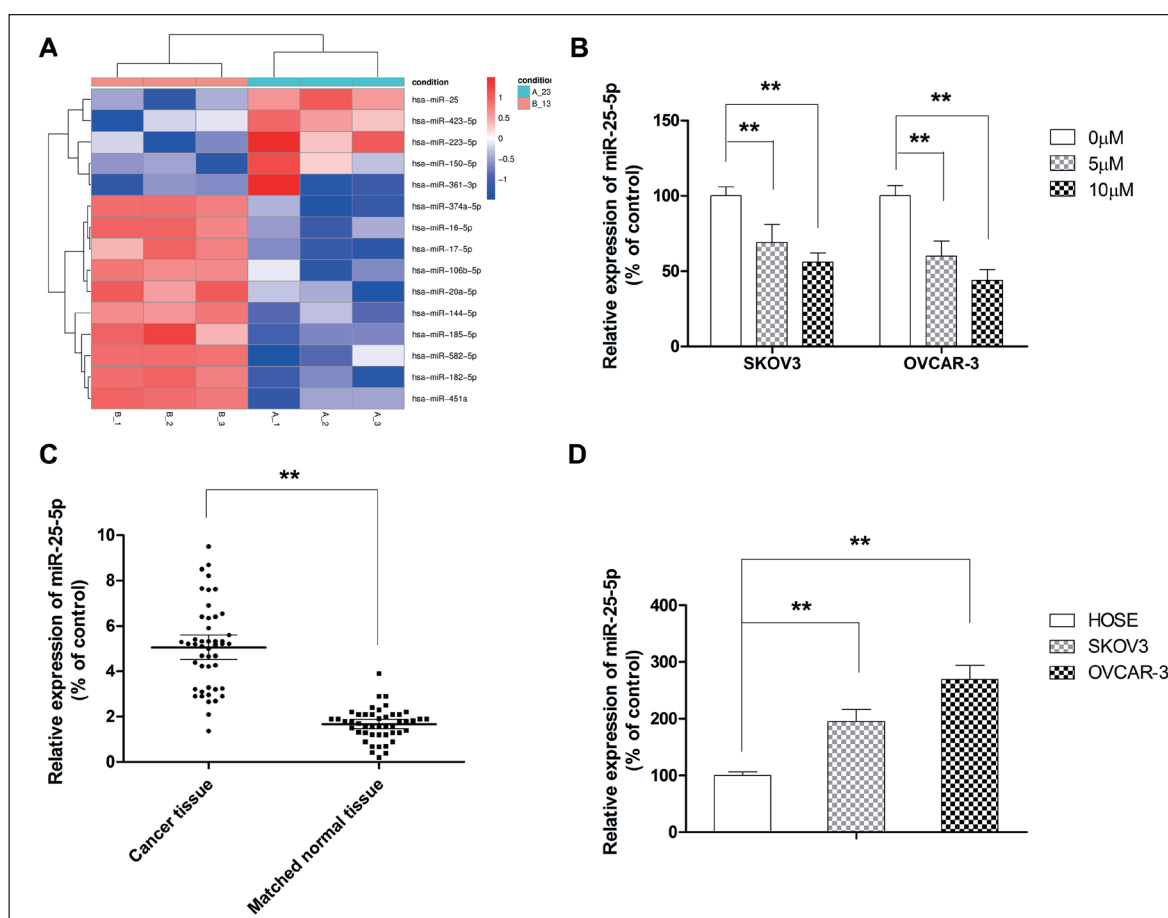


**Figure 4.** PG downregulates miR-25 in ovarian cancer cells. *A*, Microarray indicated that PG treatment led to downregulation of miR-25. *B*, miR-25 expression was dose-dependently suppressed by PG treatment. *C*, miR-25 was abnormally highly expressed in cancer tissues compared with normal tissues. *D*, miR-25 was aberrantly high expressed in ovarian cancer cells compared with normal cells.  $**p < 0.01$ .

5C, the wound closure inhibition of ovarian cancer cells was significantly compromised by ectopic miR-25 expression. Meanwhile, the invasive cell number was also increased in SKOV3 and OVCAR-3 cells with miR-25 overexpression (Figure 5E). The effect of PG on MMP-2 and TIMP-3 expression in both ovarian cancer cells was also markedly reversed by ectopic miR-25 expression (Figure 5F). Taken together, our results indicated that ectopic miR-25 expression could attenuate the anti-cancer activities of PG against ovarian cancer.

#### ***Silencing miR-25 Expression in Ovarian Cancer Cells Augments the Anti-Cancer Activities of PG***

After transfection of cells with miR-25 inhibitor, the level of miR-25 expression was decreased by about a half (Figure 6A). Then whether miR-25 knockdown affected the pro-apoptotic activi-

ties of PG was examined. Our results indicated that apoptotic cell population was respectively increased to about 30% and 35% by miR-25 knockdown in SKOV3 and OVCAR-3 cells (Figure 6B). The expression levels of apoptotic markers were also examined. The activation of caspase-3 and PARP was markedly enhanced by miR-25 knockdown. PG-induced downregulation of Bcl-2 was significantly augmented in SKOV3 and OVCAR-3 cells with miR-25 knockdown (Figure 6C). Meanwhile, the upregulation caused by PG treatment was also enhanced by miR-25 knockdown (Figure 6D). The effect of miR-25 knockdown on cell migration and invasion was also evaluated. As shown in Figure 6C, the wound closure inhibition of ovarian cancer cells was significantly enhanced by miR-25 knockdown. Meanwhile, miR-25 knockdown significantly reduced the number of invasive cells (Figure 6E). The effect of PG on MMP-2 and TIMP-3 expression

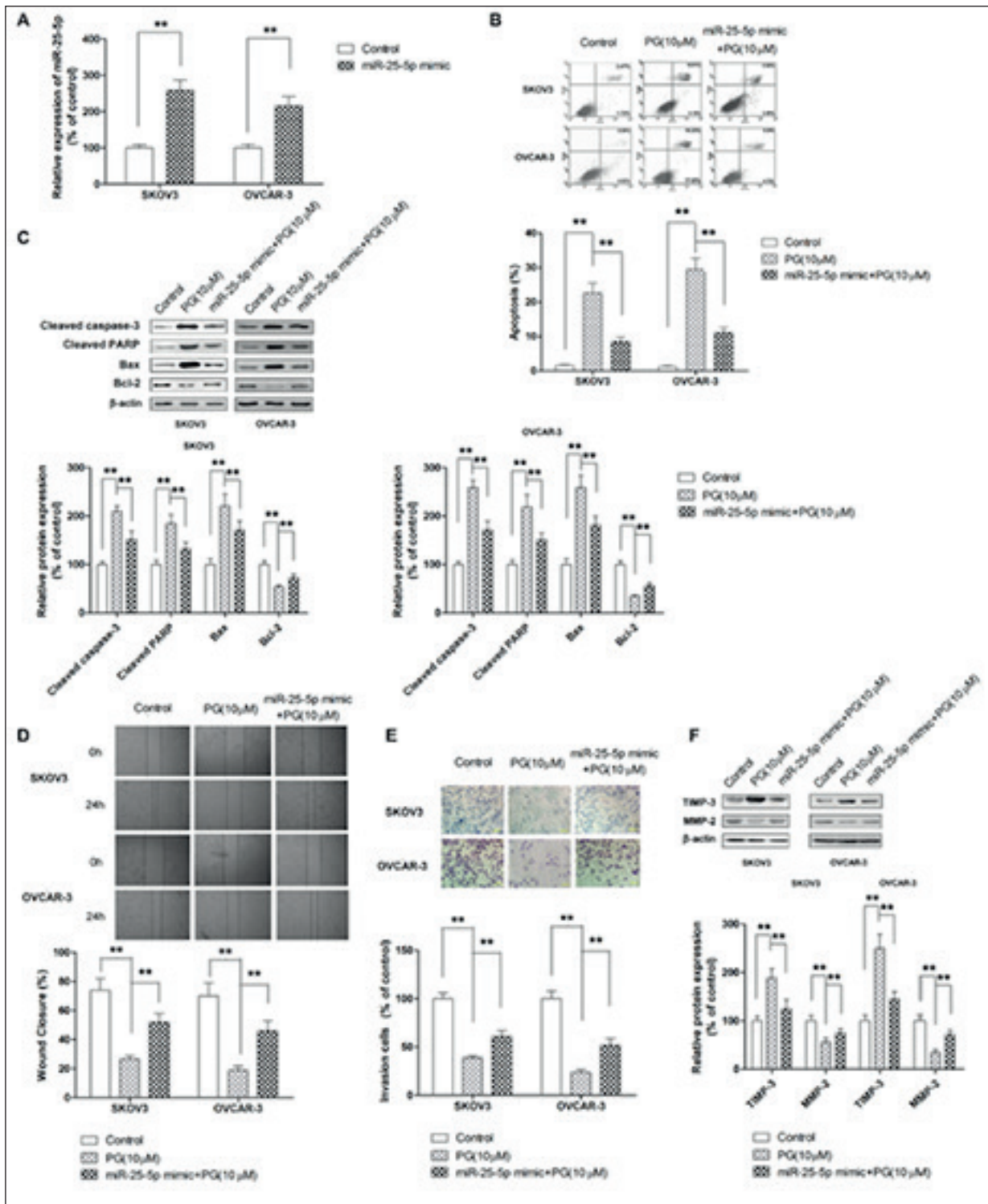


**Figure 5.** Forced miR-25 expression compromises the anti-cancer activities of PG. Transfection of SKOV3 and OVCAR-3 cells with miR-25 mimic followed by treatment of cells with 10  $\mu$ M PG. **A**, qRT-PCR assessed the expression level of miR-25. **B**, Apoptosis was determined by flow cytometry. **C**, The expression levels of cleaved caspase-3, cleaved PARP, Bax and Bcl-2 were assessed by Western blot. **D**, Cell migration was assessed by wound healing assay. **E**, Cell invasion was assessed by transwell assay. **F**, The expression levels of MMP-2 and TIMP-3 were assessed by Western blot. \*\* $p < 0.01$ .

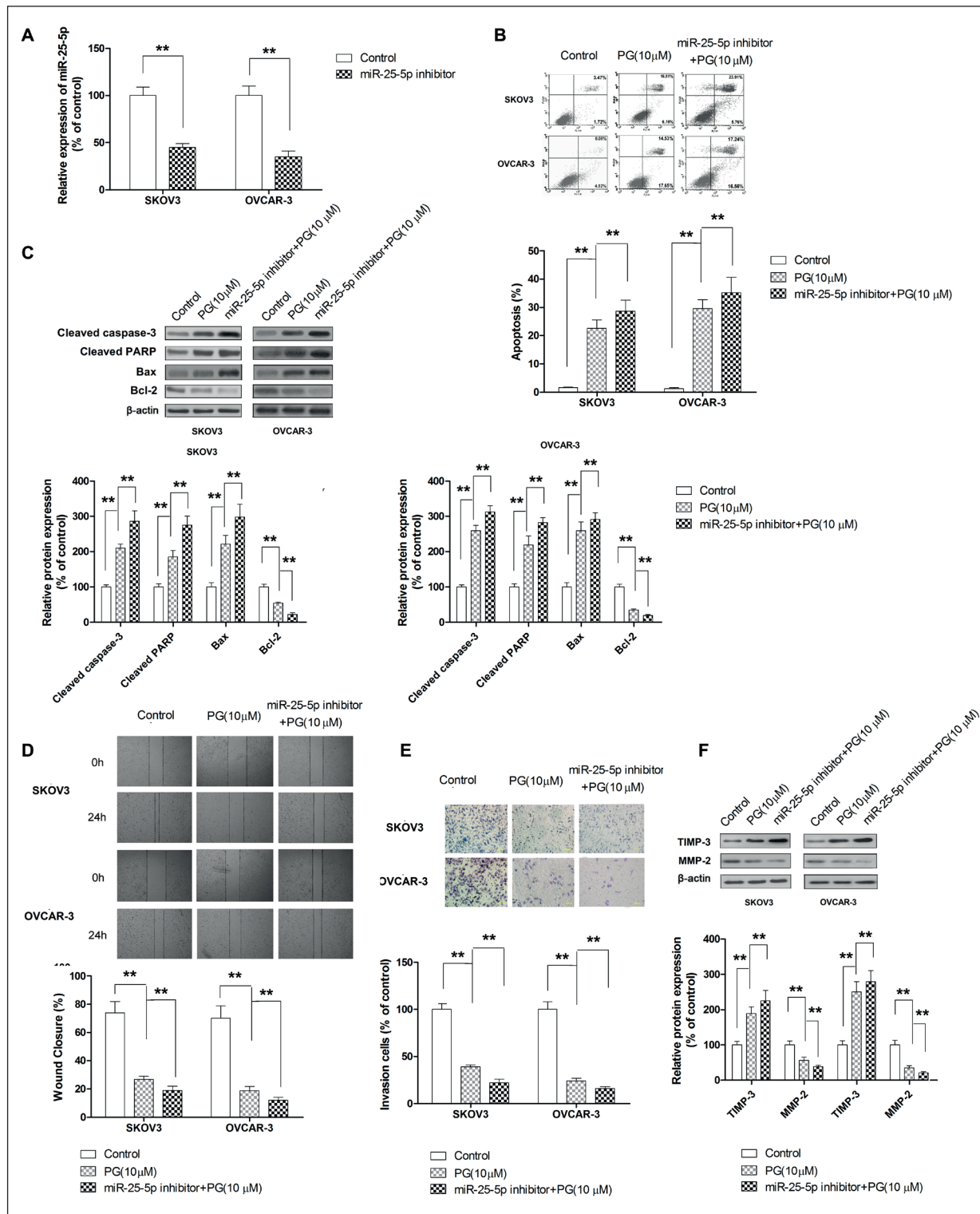


**Figure 6.** Silencing miR-25 expression augments the anti-cancer activities of PG. Transfection of SKOV3 and OVCAR-3 cells with miR-25 inhibitor followed by treatment of cells with 10 μM PG. **A**, qRT-PCR assessed the expression level of miR-25. **B**, Apoptosis was detected by flow cytometry. **C**, The expression levels of cleaved caspase-3, cleaved PARP, Bax and Bcl-2 were assessed by Western blot. **D**, Cell migration was assessed by wound healing assay. **E**, Cell invasion was assessed by transwell assay. **F**, The expression levels of MMP-2 and TIMP-3 were assessed by Western blot. \*\*  $p < 0.01$ .

in both ovarian cancer cells was also markedly augmented by miR-25 knockdown (Figure 6F). Taken together, our results indicated that miR-25 knockdown enhances the anti-cancer activities of PG against ovarian cancer.

## Discussion

Accumulating evidence has indicated that a variety of natural compounds could exhibit potent anti-cancer activities against human malignancies. More importantly, natural compounds are generally well tolerated compared with conventional chemotherapeutic agents<sup>10</sup>. As early as 2014, PG has been found to promote apoptosis and block cell cycle in lung cancer cells<sup>17</sup>. A recent study by Du et al<sup>10</sup> showed that the anti-cancer activities of PG against lung cancer were attributed to its modulation of PPAR $\gamma$  signaling. The effect of PG on apoptosis induction has also been reported by different research groups<sup>18-20</sup>. In oral squamous cell carcinoma, surviving has been reported to be the primary target of PG<sup>18</sup>. Interestingly, miR-27 and miR-124 have been identified as the molecular target mediating the anti-cancer activities of PG in osteosarcoma and melanoma cells, respectively<sup>19,20</sup>. This evidence suggested the ability of PG to modulate the expression of miRNAs. We indicated that PG was able to exhibit anti-growth activities and cause cell cycle blockade. In addition, our findings indicated that PG suppressed the metastasis of ovarian cancer cells via inhibiting cell migration and invasion. Microarray results showed that PG exhibited anti-cancer activities by modulating miR-25 in ovarian cancer cells. Altogether, these findings showed that PG might be able to exhibit anti-cancer activities by regulating the expression of onco-miRNAs.

Located in intron 13 of the MCM7 oncogene on chromosome 7q22.1c, miR-25 belongs to the same family with other two miRNAs, miR-106b and miR-93<sup>21</sup>. The involvement of miR-25 in human malignancies has been confirmed in various studies<sup>22,23</sup>. However, the role of miR-25 in the development and progression is differentiated depending on cancers derived from a different origin. In melanoma, miR-25 has been found to play a role as oncogene by targeting RNA binding motif protein 47<sup>24</sup>. In non-small cell lung cancer, miR-25 has been reported to enhance migratory and invasive capability by targeting KLF4<sup>25</sup>. Besides, the mediating role of miR-25 in chemoresis-

tance has also been evidenced in gastric cancer<sup>26</sup>. On the contrary, in Chen et al<sup>27</sup> study, miR-25 has been found to exhibit anti-proliferative and anti-metastatic activities in osteosarcoma. A recent study has also found that miR-25 could suppress the metastatic potential of cisplatin-resistance cervical cancer cells<sup>28</sup>. In terms of ovarian cancer, the pro-survival role of miR-25 was firstly reported in 2012<sup>29</sup>. The prognosis of miR-25 has been analyzed in 86 patients, showing that aberrantly high expression of miR-25 correlates with shorter overall survival<sup>30</sup>. Large tumor suppressor 2 (LATS2) was identified as a target of miR-25 and responsible for its pro-proliferative effect on ovarian cancer cells<sup>31</sup>. Downregulation of miR-25 has also been found to suppress cell proliferation and invasion in ovarian cancer cells<sup>32</sup>. These combined results showed that miR-25 functioned as oncogene in ovarian cancer and can be considered as a therapeutic target. Our results indicated that the anti-cancer activities of PG against ovarian cancer cells were associated with downregulation of miR-25. Ectopic miR-25 expression was able to significantly compromise the anti-cancer activities of PG while miR-25 knockdown could enhance the anti-cancer activities of PG. Therefore, our results offered experimental evidence that miR-25 was a key therapeutic target of PG and further supported the role of miR-25 as oncogene in ovarian cancer.

## Conclusions

We indicated that PG could exhibit anti-cancer activities in ovarian cancer *in vitro* and its anti-cancer activities were mediated by its downregulation of miR-25.

## Conflict of Interest

The Authors declare that they have no conflict of interests.

## References

- 1) LUO L, YQ GAO, XF SUN. Circular RNA ITCH suppresses proliferation and promotes apoptosis in human epithelial ovarian cancer cells by sponging miR-10a-alpha. *Eur Rev Med Pharmacol Sci* 2018; 22: 8119-8126.
- 2) OZOLS RF. Treatment goals in ovarian cancer. *Int J Gynecol Cancer* 2005; 15 Suppl 1: 3-11.
- 3) YAO N, YU L, ZHU B, GAN HY, GUO BQ. LncRNA GI-HCG promotes development of ovarian cancer by

- regulating microRNA-429. *Eur Rev Med Pharmacol Sci* 2018; 22: 8127-8134.
- 4) AHMAD S, QURESHI AN, KAZMI A, RASOOL A, GUL M, ASHFAQ M, BATOOL L, REHMAN RA, AHMAD J, MUNIBA. First cancer statistics report from Hazara division. *J Ayub Med Coll Abbottabad* 2013; 25: 71-73.
  - 5) GUO TY, XU HY, CHEN WJ, WU MX, DAI X. Down-regulation of miR-1294 associates with prognosis and tumor progression in epithelial ovarian cancer. *Eur Rev Med Pharmacol Sci* 2018; 22: 7646-7652.
  - 6) VENTURA A, JACKS T. MicroRNAs and cancer: short RNAs go a long way. *Cell* 2009; 136: 586-591.
  - 7) SUO HB, ZHANG KC, ZHAO J. MiR-200a promotes cell invasion and migration of ovarian carcinoma by targeting PTEN. *Eur Rev Med Pharmacol Sci* 2018; 22: 4080-4089.
  - 8) ZHANG S, ZHANG JY, LU LJ, WANG CH, WANG LH. MiR-630 promotes epithelial ovarian cancer proliferation and invasion via targeting KLF6. *Eur Rev Med Pharmacol Sci* 2017; 21: 4542-4547.
  - 9) LEE H, KIM NH, YANG H, BAE SK, HEO Y, CHOUDHARY I, KWON YC, BYUN JK, YIM HJ, NOH BS, HEO JD, KIM E, KANG C. The hair growth-promoting effect of Rumex japonicus Houtt. Extract. *Evid Based Complement Alternat Med* 2016; 2016: 1873746.
  - 10) DU Y, LV Z, SUN D, LI Y, SUN L, ZHOU J. Physcion 8-O-beta-glucopyranoside exerts anti-tumor activity against non-small cell lung cancer by targeting PPAR $\gamma$ . *Anat Rec (Hoboken)* 2018 Oct 12. doi: 10.1002/ar.23975. [Epub ahead of print]
  - 11) HAN J, ZHAO P, SHAO W, WANG Z, WANG F, SHENG L. Physcion 8-O-beta-glucopyranoside exhibits anti-leukemic activity through targeting sphingolipid rheostat. *Pharmacol Rep* 2018; 70: 853-862.
  - 12) WANG Q, YAN Y, ZHANG J, GUO P, XING Y, WANG Y, QIN F, ZENG Q. Physcion 8-O-beta-glucopyranoside inhibits clear-cell renal cell carcinoma by downregulating hexokinase II and inhibiting glycolysis. *Biomed Pharmacother* 2018; 104: 28-35.
  - 13) LI W, LI F, ZHU Y, SONG D. Physcion 8-O-beta-glucopyranoside regulates cell cycle, apoptosis, and invasion in glioblastoma cells through modulating Skp2. *Biomed Pharmacother* 2017; 95: 1129-1138.
  - 14) WANG Q, JIANG Y, GUO R, LV R, LIU T, WEI H, MING H, TIAN X. Physcion 8-O-beta-glucopyranoside suppresses tumor growth of hepatocellular carcinoma by downregulating PIM1. *Biomed Pharmacother* 2017; 92: 451-458.
  - 15) WANG Q, WANG Y, XING Y, YAN Y, GUO P, ZHUANG J, QIN F, ZHANG J. Physcion 8-O-beta-glucopyranoside induces apoptosis, suppresses invasion and inhibits epithelial to mesenchymal transition of hepatocellular carcinoma HepG2 cells. *Biomed Pharmacother* 2016; 83: 372-380.
  - 16) HUANG D, CUI L, AHMED S, ZAINAB F, WU Q, WANG X, YUAN Z. An overview of epigenetic agents and natural nutrition products targeting DNA methyltransferase, histone deacetylases and microRNAs. *Food Chem Toxicol* 2019; 123: 574-594.
  - 17) XIE QC, YANG YP. Anti-proliferative of physcion 8-O-beta-glucopyranoside isolated from Rumex japonicus Houtt. on A549 cell lines via inducing apoptosis and cell cycle arrest. *BMC Complement Altern Med* 2014; 14: 377.
  - 18) LIU MD, XIONG SJ, TAN F, LIU Y. Physcion 8-O-beta-glucopyranoside induces mitochondria-dependent apoptosis of human oral squamous cell carcinoma cells via suppressing survivin expression. *Acta Pharmacol Sin* 2016; 37: 687-697.
  - 19) WANG Z, YANG H. EMMPRIN, SP1 and microRNA-27a mediate physcion 8-O-beta-glucopyranoside-induced apoptosis in osteosarcoma cells. *Am J Cancer Res* 2016; 6: 1331-1344.
  - 20) ZHANG D, HAN Y, XU L. Upregulation of miR-124 by physcion 8-O-beta-glucopyranoside inhibits proliferation and invasion of malignant melanoma cells via repressing RLIP76. *Biomed Pharmacother* 2016; 84: 166-176.
  - 21) PETROCCA F, VECCHIONE A, CROCE CM. Emerging role of miR-106b-25/miR-17-92 clusters in the control of transforming growth factor beta signaling. *Cancer Res* 2008; 68: 8191-8194.
  - 22) FUJIWARA T, UOTANI K, YOSHIDA A, MORITA T, NEZU Y, KOBAYASHI E, YOSHIDA A, UEHARA T, OMORI T, SUGIU K, KOMATSUBARA T, TAKEDA K, KUNISADA T, KAWAMURA M, KAWAI A, OCHIYA T, OZAKI T. Clinical significance of circulating miR-25-3p as a novel diagnostic and prognostic biomarker in osteosarcoma. *Oncotarget* 2017; 8: 33375-33392.
  - 23) CASADEI L, CALORE F, CREIGHTON CJ, GUESCINI M, BATTE K, IWENOFU OH, ZEWDU A, BRAGGIO DA, BILL KL, FADDA P, LOVAT F, LOPEZ G, GASPARINI P, CHEN JL, KLDADNEY RD, LEONE G, LEV D, CROCE CM, POLLOCK RE. Exosome-derived miR-25-3p and miR-92a-3p stimulate liposarcoma progression. *Cancer Res* 2017; 77: 3846-3856.
  - 24) JIANG QQ, LIU WB. miR-25 promotes melanoma progression by regulating RNA binding motif protein 47. *Med Sci (Paris)* 2018; 34: 59-65.
  - 25) DING X, ZHONG T, JIANG L, HUANG J, XIA Y, HU R. miR-25 enhances cell migration and invasion in non-small-cell lung cancer cells via ERK signaling pathway by inhibiting KLF4. *Mol Med Rep* 2018; 17: 7005-7016.
  - 26) HE J, QI H, CHEN F, CAO C. MicroRNA-25 contributes to cisplatin resistance in gastric cancer cells by inhibiting forkhead box O3a. *Oncol Lett* 2017; 14: 6097-6102.
  - 27) CHEN B, LIU J, QU J, SONG Y, LI Y, PAN S. MicroRNA-25 suppresses proliferation, migration, and invasion of osteosarcoma by targeting SOX4. *Tumour Biol* 2017; 39: 1010428317703841.
  - 28) SONG J, LI Y. miR-25-3p reverses epithelial-mesenchymal transition via targeting Sema4C in cisplatin-resistance cervical cancer cells. *Cancer Sci* 2017; 108: 23-31.

- 29) ZHANG H, ZUO Z, LU X, WANG L, WANG H, ZHU Z. MiR-25 regulates apoptosis by targeting Bim in human ovarian cancer. *Oncol Rep* 2012; 27: 594-598.
- 30) WANG X, MENG X, LI H, LIU W, SHEN S, GAO Z. MicroRNA-25 expression level is an independent prognostic factor in epithelial ovarian cancer. *Clin Transl Oncol* 2014; 16: 954-958.
- 31) FENG S, PAN W, JIN Y, ZHENG J. MiR-25 promotes ovarian cancer proliferation and motility by targeting LATS2. *Tumour Biol* 2014; 35: 12339-12344.
- 32) LIU D, LIU T, TENG Y, CHEN W, ZHAO L, LI X. Ginsenoside Rb1 inhibits hypoxia-induced epithelial-mesenchymal transition in ovarian cancer cells by regulating microRNA-25. *Exp Ther Med* 2017; 14: 2895-2902.